Published in "Nuclear Physics A 796(1-4): 1-10, 2007"
which should be cited to refer to this work.

Nanosecond lifetimes and electromagnetic transition strengths in ^{196}Au

P. Petkov [a,*], J. Jolie [b], S. Heinze [b], S.E. Drissi [c], M. Dorthe [c], J. Gröger [c], J.L. Schenker [c]

[a] *Bulgarian Academy of Sciences, Institute for Nuclear Research and Nuclear Energy, Tzarigradsko chaussee 72, 1784 Sofia, Bulgaria*
[b] *Institut für Kernphysik der Universität zu Köln, 50937 Köln, Germany*
[c] *Physics Department, University of Fribourg, CH-1700 Fribourg, Switzerland*

Abstract

Nanosecond lifetime measurements were performed in ^{196}Au by means of the pulsed-beam technique. Using the centroid-shift method, one new lifetime has been determined and three known have been re-measured. The data for the transition probabilities are compared to the predictions of the extended supersymmetry for ^{196}Au. The comparison reveals a partial agreement, which can be considered as a success for the theory describing the complicated structure of the odd–odd nucleus.

PACS: 21.10.Tg; 23.20.Lv; 27.80.+w

Keywords: NUCLEAR REACTIONS ^{196}Pt(d, 2n), $E = 12.2$ MeV; measured E_γ, I_γ, $\gamma(t)$; ^{196}Au levels deduced τ, $B(\lambda)$. Enriched target, Ge detector, centroid-shift analysis, comparison with extended supersymmetry

1. Introduction

Almost 15 years after its introduction in nuclear physics [1], Metz et al. [2] presented strong evidence for the existence of extended supersymmetry in atomic nuclei, by a detailed study of ^{196}Au. Following the introduction of dynamical supersymmetries in nuclear physics by Iachello [3], this extended supersymmetry (or neutron–proton supersymmetry) deals with boson–

fermion and neutron–proton degrees of freedom. The extended supersymmetry relates excitations occurring in a quartet of nuclei consisting of an even–even nucleus with $(\mathcal{N}_\nu + \mathcal{N}_\pi)$ bosons, an odd-proton and an odd-neutron nucleus, both with $(\mathcal{N}_\nu + \mathcal{N}_\pi) - 1$ bosons and an odd–odd nucleus with $(\mathcal{N}_\nu + \mathcal{N}_\pi) - 2$ bosons. The extended supersymmetry relates the often very complex structure of the odd–odd nucleus to the simpler ones of even–even and odd-A systems. The formalism of the $U_\nu(6/12) \otimes U_\pi(6/4)$ extended supersymmetry is described in Refs. [1,4,5]. To be applicable for the $U_\nu(6/12) \otimes U_\pi(6/4)$ scheme, the even–even core should exhibit the O(6) symmetry of the IBM. The odd proton has to occupy a dominant $j = 3/2$ orbit and the odd neutron the $j = 1/2$, $3/2$ and $5/2$ orbits. These constraints are fulfilled in the Au, Ir region for the negative-parity states formed by the $\nu(3p_{1/2}, 3p_{3/2}, 2f_{5/2}) \times \pi 2d_{3/2}$ configurations [1,2,5,6].

The evidence for extended supersymmetry was obtained from the study of the odd–odd nucleus ^{196}Au in ^{197}Au($\vec{\mathrm{d}}$, t), ^{197}Au(p, d) and ^{198}Hg($\vec{\mathrm{d}}$, α) transfer reactions [2]. Within the framework of extended supersymmetry, the low-lying part of the negative parity spectrum of odd–odd ^{196}Au follows as a prediction from the reproduction of the spectra of ^{194}Pt within the O(6), of ^{195}Au within the U(6/4) proton- and of ^{195}Pt within the U(6/12) neutron-supersymmetry. In all three cases, of course, the even–even nucleus is treated in the same way. In the model, three parameters determine the structure of ^{194}Pt, two more are needed to reproduce in addition ^{195}Pt, and a sixth to determine also ^{195}Au. All six parameters then yield a prediction for ^{196}Au.

In parallel to the transfer work several in-beam γ-ray and conversion electron studies were performed to further study ^{196}Au. One of these studies relying on a pulsed beam is presented here. Earlier in-beam work can be found in Ref. [7]. Finally, besides the (p, d) and polarized ($\vec{\mathrm{d}}$, t) reactions, also the ($\vec{\mathrm{d}}, \alpha$) transfer reaction was used to improve the knowledge on excited states in ^{196}Au [8] and to compare with the expectation for the ($\vec{\mathrm{d}}, \alpha$) reactions within the dynamical supersymmetry [9].

Following the discussion in the previous studies, almost all states below 500 keV can be considered to be well established. However, while energies, spins and parities are well established little knowledge of electromagnetic decays is available. In this paper we report on a study of lifetimes in ^{196}Au measured by the centroid shift method and compare the extracted transition strengths to the supersymmetric predictions.

2. Experiments and data analysis

Delayed coincidences with a pulsed beam were measured in the ^{196}Pt(d, 2nγ)^{196}Au reaction at the Phillips Cyclotron of the Paul Scherrer Institute. The beam energy was $E = 12.2$ MeV. A 10 mg/cm^2 foil enriched to 97% in ^{196}Pt was used a target.

The STOP pulses for the TAC were provided by the beam reference frequency (r.f.) of 5.19 MHz, whereby an electrostatic deflector suppressed 3 out of 4 beam bursts. The START signals originated from a germanium detector with a volume of about 19 cm^3 placed in the large anti-Compton spectrometer [10]. The amplification of the detector was set in such a way that γ-ray energies up to 650 keV were measured. The germanium detector was positioned at 90° with respect to the beam axis. A γ-ray spectrum recorded in coincidence with the full TAC region ($\approx$ 200 ns) is displayed in Fig. 1.

The setup ensured an integral time resolution of about 20 ns which for higher γ-ray energies reached less than 10 ns. A time-energy matrix (1024 × 4096 channels) was constructed off-line. The matrix was first used to produce time-related (prompt and delayed) germanium γ-ray spectra by setting cuts with windows on the time axis. These spectra were employed for an inspection of the data for long-lived isomers. Then, windows were set on the energy axis on full-energy

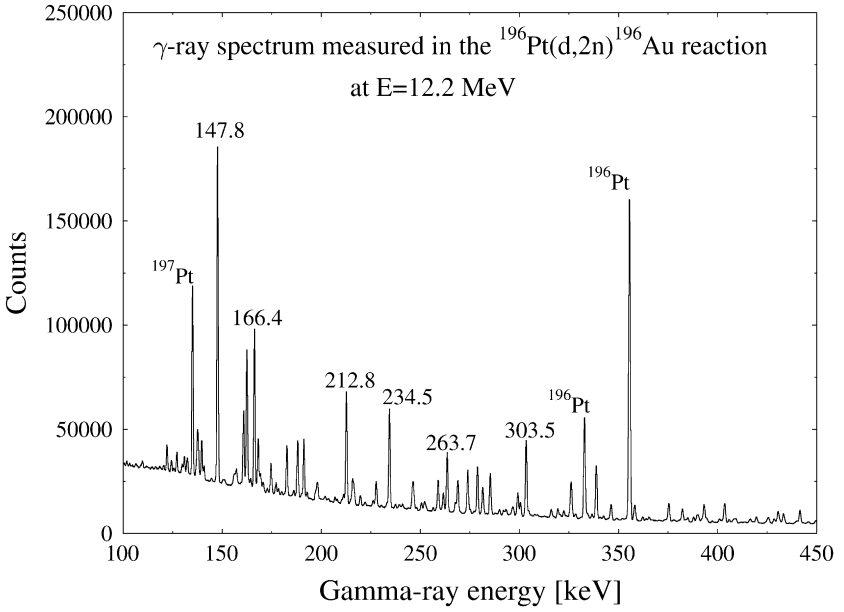

Fig. 1. γ-ray spectrum measured in coincidence with the full TAC time range. Transitions in ^{196}Au are indicated by their energy in keV. Strong transitions from other reaction channels are labelled by the deexcited nucleus.

peaks as well as on neighboring Compton background. Net time distributions of γ-ray transitions corresponding to full-energy peaks were obtained after subtraction of random coincidences and Compton-background time contributions. More details on the analyzing procedure (the generalized centroid-shift method) can be found in Refs. [11–13] and references therein. Here, we briefly describe its main features.

To obtain the Compton background contribution to the time distribution of a given photo-peak, we interpolate time distributions corresponding to background windows set on both sides of the photo-peak in the energy spectrum. Then, the interpolated time distribution is subtracted from that of the photo-peak time distribution. After the additional subtraction of the random coincidences, the centroids (first moments, time centroids) of the net time distributions are plotted versus γ-ray energy thus producing a centroid diagram. A zero-time line is formed by the time centroids of prompt transitions. Deviations from the smooth zero-time line indicate delayed transitions. In the case of absence of contaminations in the particular γ-ray line selected, these deviations provide a measure of the effective lifetimes of the corresponding nuclear levels. However, in some situations a uniform choice for the selection of the summation limits used for the determination of the centroids of all net time distributions may be quite difficult. Therefore we preferred to use the centroid diagram as a first indication of measurable lifetimes. At a second stage, we interpolated a prompt reference curve among the ones whose centroids are lying on the zero-time line and compared it to the corresponding delayed time curve. Then, the full statistics of both curves was used to determine the prompt and the delayed centroids. The graphical comparison of the prompt and delayed curves helps to identify cases where undesired prompt admixtures are present into the time distributions. With our setup, this arises when a gate in the γ-ray spectrum is set on a doublet (multiplet) of transitions among which the prompt ones predominate. Such cases were treated according to Ref. [12], where we discuss in detail the oc-

currence of undesired prompt admixtures and a procedure for their elimination. An additional problem can appear when the level investigated is fed by delayed transitions with effective delay(s) τ_D^i and intensities I_D^i. If $\tau_D^i \ll \tau_{\rm eff}$ where $\tau_{\rm eff}$ is the effective lifetime of the depopulating transition, i.e., of the level investigated, the delayed feeding can be neglected. If $\tau_D^i \geqslant \tau_{\rm eff}$ one may use the relation

$$\tau_{\rm eff} = \tau_{\rm lev} + \frac{\sum_i \tau_D^i I_D^i}{I_{\rm tot}}, \tag{1}$$

where $I_{\rm tot}$ is the total depopulating intensity and $\tau_{\rm lev}$ is the "true" lifetime of the level to be determined (cf. also Ref. [13]). Thus, the determination of $\tau_{\rm lev}$ is only possible if the intensities and the effective delays of all feeding transitions are known unless a coincidence method is applied. To increase the statistics of the data to be analyzed we compressed four times the time distributions originally measured on 1024 channels.

3. Results

The centroid diagram from the present analysis is displayed in Fig. 2. We estimate that the precision of the constructed zero-time line is about 0.3 ns. This conservative estimate is due mainly to the behavior of the time distributions below 130 keV which is characterized by a significant (time) walk. The necessary level scheme informations for the considerations were taken from Refs. [7,8,14] to which the reader is referred for more details. For the construction of the zero-time line we used mainly centroids of γ-transitions in ^{196}Au determined with good statistics and forming a smooth line. No lifetime information is available for the corresponding levels but the assumption that all of them have by our setup measurable and almost equal lifetimes is very unlikely. The agreement found below for the case of previously known lifetimes strengthen our conviction that the zero-time line is correctly constructed.

In Fig. 2, several centroids deviate from the zero-time line interconnecting the centroids of the prompt transitions. These are the centroids of the 148, 188, 213, 257 and 292 keV transitions. The centroid of the 426 keV transitions from the level at 657.8 keV (cf. Ref. [7]) also deviates somewhat from the zero-time line, but the statistics of the corresponding time distribution allows only to set the upper limit:

$$\tau\,(657.8\ \text{keV}) \leqslant 2.4\ \text{ns}.$$

The $I^\pi = 7^+$ level at 232.5 keV is an already known [14] isomer with $\tau = 2.38\ (22)$ ns. Our result for the effective lifetime of that level from the centroid-shift analysis illustrated in Fig. 3 is $\tau_{\rm eff} = 2.43\ (11)$. The agreement is impressive, but this is misleading because the level at 232.5 keV is fed via the transition of 188 keV by another isomer, namely the 8^+ level at 420.7 keV. The old result [14] for the lifetime τ of this isomer is 2.89 (29) ns. Our lifetime analysis, illustrated in Fig. 4, points to a value of:

$$\tau\,(8^+\ \text{at}\ 420.7\ \text{keV}) = 3.26\ (20)\ \text{ns},$$

which coincides within the error bars with the old result. No delayed feeding could be identified for the 420.7 keV level. This level feeds the 7^+ level at 232.5 keV both directly and indirectly. The feeding has to be taken into account in the lifetime analysis for the 232.5 keV level. For this purpose, we used the relative intensities of the transitions in the cascades leading to the 232.5 keV as given in Ref. [14] (including internal conversion), and the areas of the 188 and 148 keV transitions derived from the spectrum shown in Fig. 1. The area of the 148 keV transition

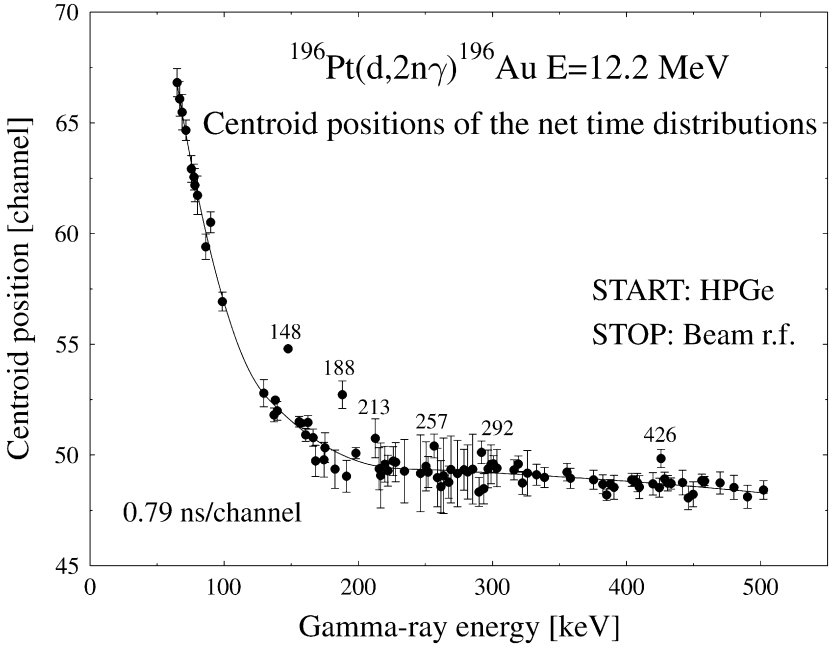

Fig. 2. Centroid diagram obtained in the present analysis. The smooth line represents the zero-time line. The centroids of the time distributions of the transitions which deviate form the zero-time line are indicated by the corresponding γ-ray energy. See also text.

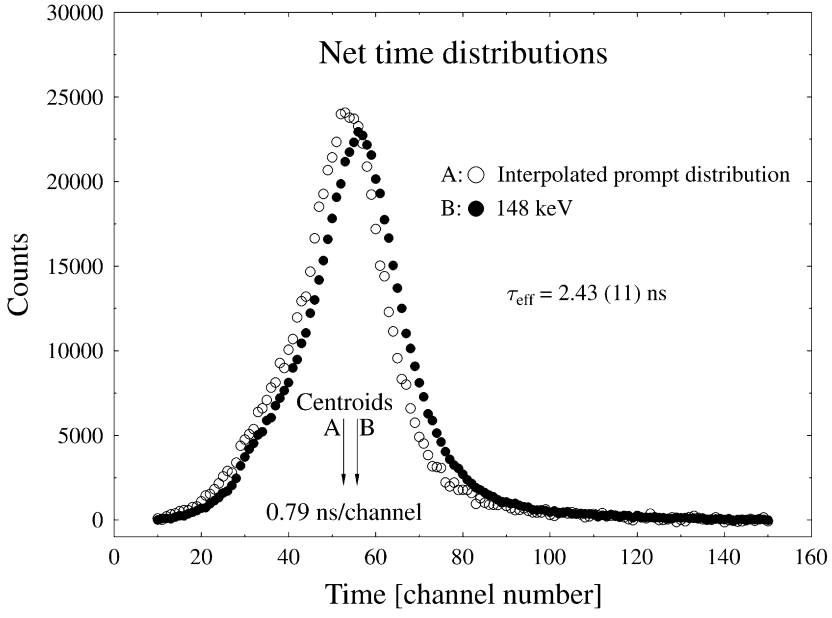

Fig. 3. Net time distribution for the centroid-shift analysis of the data for the 148 keV transition. The interpolated prompt time distribution is also show. The prompt and delayed centroids are indicated by arrows.

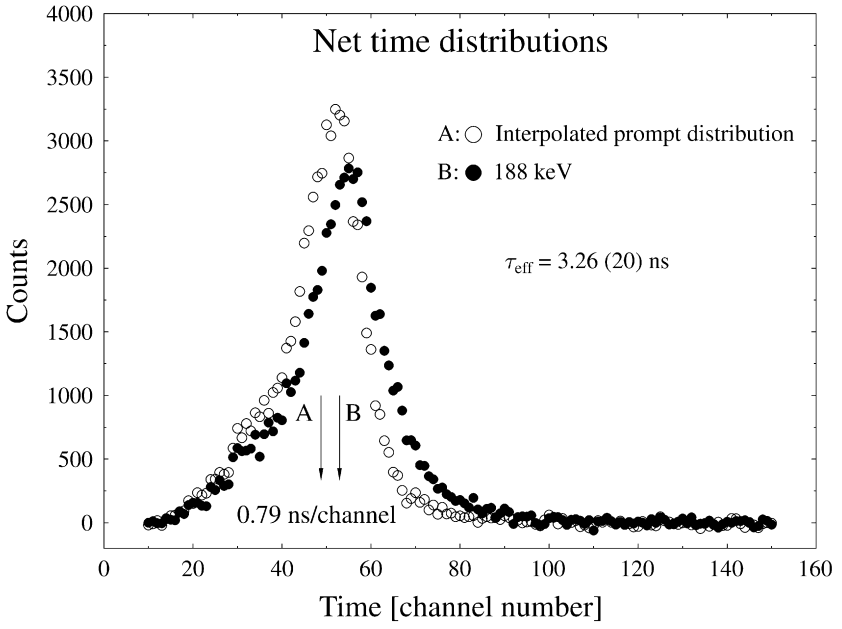

Fig. 4. Centroid-shift analysis of the data for the 188 keV transition. See also caption to Fig. 3.

is about five time larger than that of the 188 keV transition. After corrections for efficiency and angular distribution effects, we applied Eq. (1) to derive for the lifetime of the 232.5 keV level:

$$\tau(7^+ \text{ at } 232.5 \text{ keV}) = 1.59\ (16) \text{ ns},$$

a value which is considerably shorter than the old result of 2.38 (22) ns.

The lifetime of the 4^- level at 212.8 keV, depopulated by a 212.8 keV transition to the ground-state, was also previously known [7] as $\tau = 2.58$ (22) ns. In our analysis, we had to take into account impurities from transitions in ^{196}Au with similar energies to that of the depopulating transition. In applying our procedure for elimination of prompt components [12], we found that about 40% of the measured time distribution are due to prompt admixtures. The results of the lifetime analysis are presented in Fig. 5. They point to a lifetime:

$$\tau(4^- \text{ at } 212.8 \text{ keV}) = 1.95\ (48) \text{ ns},$$

since no delayed feeding could be found. This value has a larger uncertainty than the old result (see above) due to the subtraction of the prompt admixtures contribution.

The centroids of the 257 and 292 keV transitions unambiguously point at a measurable lifetime of the $I^\pi = 1^-, 2^-$ level at 298.5 keV (cf. Ref. [7]). The time distribution of the 257 keV transition contains some impurities. Therefore we present in Fig. 6 the results of the lifetime analysis for the 292 keV transition. Because no delayed feeding could be identified, they indicate a lifetime of:

$$\tau(1^-, 2^- \text{ at } 298.5 \text{ keV}) = 0.8\ (4) \text{ ns}.$$

This lifetime is determined for the first time.

For the other levels in ^{196}Au observed in our experiment, an upper limit for the lifetimes $\tau \leqslant 0.4$ ns can be set. It should be mentioned here that the lifetimes derived above in the present

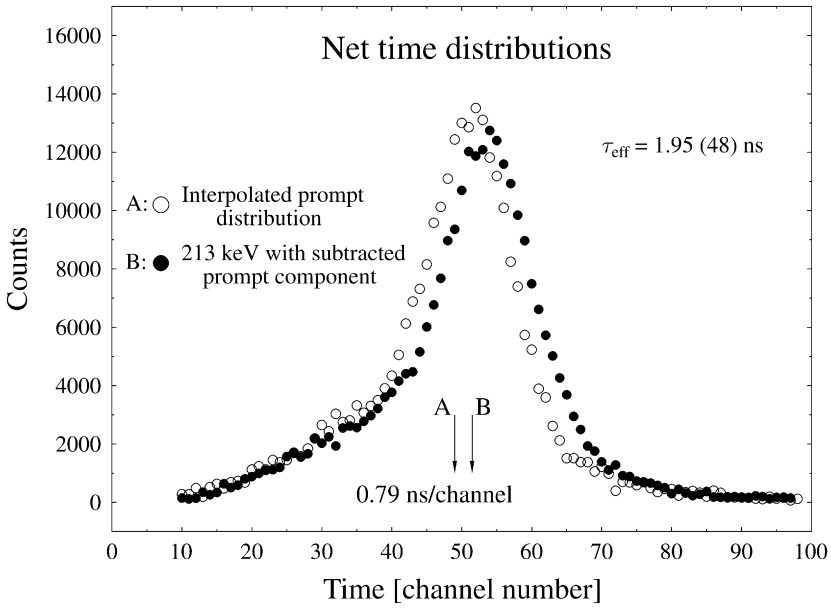

Fig. 5. Centroid-shift analysis of the data for the 213 keV transition. The data were corrected for the presence of prompt admixtures. See also caption to Fig. 3.

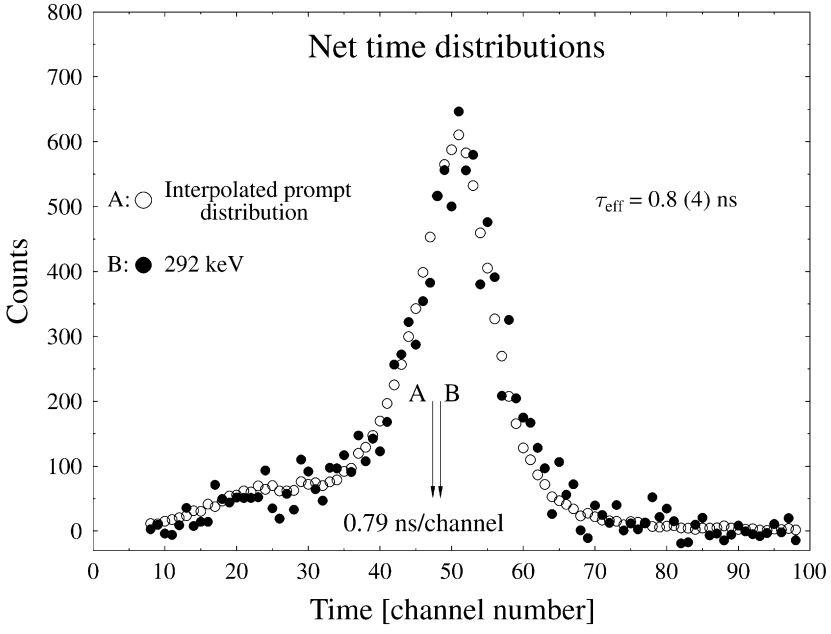

Fig. 6. Centroid-shift analysis of the data for the 292 keV transition. See also caption to Fig. 3.

work are not completely free from the problem of a possible unobserved delayed feeding. The latter can be related to low-intensity γ-ray transitions from higher-lying isomers or to internal

Table 1
Reduced transition probabilities derived from the lifetimes in the present work. Additional spectroscopic data were taken from Refs. [7,8,14]. Electric reduced transition probabilities are presented in units of e^2b^λ and magnetic ones (M1) in units of μ_N^2, respectively. For the 1^- level at 298.5 keV, two sets of data are presented, one assuming that most depopulating transitions are M1, and the other-E2. Three hypotheses are considered for the 425.4 keV transition which depopulates the level with unknown spin at 657.8 keV, namely for M1, E2 and E1 character. For transitions between states with negative parity we also give the theoretical values

$E_{\rm lev}$ [keV]	I_i^π	E_γ [keV]	I_f^π	$\sigma\lambda$	$B(\sigma\lambda)$	$B(\sigma\lambda)$ [W.u.]	$B(\sigma\lambda)$ [W.u.] SUSY
232.5	7^+	147.8	5^+	E2	0.34(4)	51(6)	
420.7	8^+	19.9	6^+	E2	0.14(5)	20(7)	
		50.6	$(6,7)^+$	(E2)	$0.52(26)\times10^{-2}$	0.77(39)	
				M1	$0.88(9)\times10^{-3}$	$0.49(5)\times10^{-3}$	
		188.2	7^+	$\delta=0.12(2)$			
				E2	$0.51(18)\times10^{-3}$	$0.76(26)\times10^{-1}$	
212.8	4^-	50.2	$2^-,3^-$	(E2)	$0.89(46)\times10^{-1}$	13.2(13.2)	0.045
		212.8	2^-	E2	$0.65(16)\times10^{-1}$	9.7(2.4)	4.7
298.5	1^-	131.2	(2^-)	M1	$0.87(50)\times10^{-3}$	$0.49(28)\times10^{-3}$	1.07×10^{-3}
		132.2	1^-	M1	$0.24(12)\times10^{-2}$	$0.13(7)\times10^{-2}$	0.14×10^{-2}
		256.6	0^-	M1	$0.55(28)\times10^{-3}$	$0.31(16)\times10^{-3}$	1.12×10^{-2}
		292.1	1^-	M1	$0.53(27)\times10^{-3}$	$0.29(15)\times10^{-3}$	7.8×10^{-3}
		298.5	2^-	M1	$0.99(55)\times10^{-4}$	$0.55(31)\times10^{-4}$	1.6×10^{-3}
		131.2	(2^-)	E2	0.10(6)	15.1(8.8)	2.5
		132.2	1^-	E2	0.28(14)	41(21)	0
		292.1	1^-	E2	$0.13(6)\times10^{-1}$	1.84(93)	0
		298.5	2^-	E2	$0.22(13)\times10^{-2}$	0.33(18)	0
657.8		425.4	7^+	M1	$\geqslant 0.27\times10^{-3}$	$\geqslant 0.15\times10^{-3}$	
		425.4	7^+	E2	$\geqslant 0.24\times10^{-2}$	$\geqslant 0.35$	
		425.4	7^+	E1	$\geqslant 0.34\times10^{-7}$	$\geqslant 0.15\times10^{-5}$	

conversion from yet unknown states. This has to be kept in mind when the data are interpreted. Only if we assume that such delayed feeding does not exist the lifetimes determined coincide with the level lifetimes $\tau_{\rm lev}$ and are not just effective values (see Eq. (1)). An argument supporting this assumption are the measurements [7] of lifetimes in ^{196}Au using conversion electrons whose results have been taken into account in our analysis.

The reduced transition probabilities derived from the lifetime data are presented in Table 1.

4. Discussion

The electromagnetic decay of the states 4^- at 212.8 keV and 1^-, 2^- at 298.5 keV can be compared with the theoretical results obtained using extended supersymmetry. The E2 operator describing the electric transition rates in the odd–odd nucleus is given by the sum of the $k=2$ generators of $\mathrm{O}^B(6)$, $\mathrm{O}_\nu^F(6)$ and $SU_\pi^F(4)$:

$$\hat{T}^{\rm E2}_m = e_b\big(s^\dagger\tilde{d}+d^\dagger s\big)^{(2)}_m + e_{f\nu}\left(\sqrt{\frac{4}{5}}\big(a^\dagger_{3/2\nu}\tilde{a}_{1/2\nu}-a^\dagger_{1/2\nu}\tilde{a}_{3/2\nu}\big)^{(2)}_m - \sqrt{\frac{6}{5}}\big(a^\dagger_{1/2\nu}\tilde{a}_{5/2\nu}-a^\dagger_{5/2\nu}\tilde{a}_{1/2\nu}\big)^{(2)}_m\right) + e_{f\pi}\big(a^\dagger_{3/2\pi}\tilde{a}_{3/2\pi}\big)^{(2)}_m. \quad (2)$$

The general operator (2) contains three effective charges which can be determined from the even–even and odd-A members of the quartet. The boson and neutron effective charge were determined from a fit to ^{194}Pt–^{195}Pt to be equal to $e_b = -e_{f\nu} = 0.15$ eb [15]. The proton effective charge was taken equal to the boson effective charge, which is the standard procedure for U(6/4) [16]. The value of $e_{f\pi} = 0.15$ eb is also very close to the one of 0.143 eb obtained from a fit of several odd proton nuclei in the Au–Ir region [17]. Using this operator the quadrupole moment of the ground-state becomes $Q(2_1^-) = -0.57$ eb which is experimentally known to be $|Q(2_1^-)| = 0.81(7)$ eb [14].

For the M1 operator we use the microscopic operator:

$$\hat{T}^{\mathrm{M1}}_m = \sqrt{\frac{3}{4\pi}}\Bigg(g_b\sqrt{10}\big(d^\dagger\tilde{d}\big)^{(1)}_m - \Sigma\sqrt{3}\Big\langle l\frac{1}{2}j_\rho \Big\| g_{l\rho}\vec{l}_\rho + g_{s\rho}\vec{s}_\rho + g_{t\rho}(Y_2\times\vec{s}_\rho)^{(1)} \Big\| l'\frac{1}{2}j'_\rho\Big\rangle \times \big(a^\dagger_{j_\rho}\tilde{a}_{j'_\rho}\big)^{(1)}_m (u_{j_\rho}u_{j'_\rho} + v_{j_\rho}v_{j'_\rho})\Bigg). \tag{3}$$

In (3) the summation runs over the single particle orbits j_ρ considered with $\rho = \nu$ and π. It is worth noticing that to employ this operator we have to use the shell model orbits $|l\frac{1}{2}j_\rho\rangle$ of the fermions. The coefficients v_j are the BCS occupation probabilities of the considered orbits with $v_j^2 + u_j^2 = 1$. In Eq. (3) the tensor part was introduced by Paar [18] to describe the core polarization [19]. The main effect of this term is that it leads to transitions between single particle states with a different value of l. Because the M1 operator contains nine parameters additional data have to be used to fix as many parameters as possible. Starting from the IBFFM calculations for ^{198}Au presented in [20] a detailed study for this nucleus was performed yielding as best g-factors: $g_b = 0.4$, $g_{l\nu} = 0$, $g_{l\pi} = 1$, $g_{s\nu} = -1.91315$ and $g_{s\pi} = 5.5857$ [21]. The g-factor of the tensor part are related to the free g_s factors by $g_{t_\rho} = 0.01\langle r^2\rangle g_{s_\rho}$ [19] leading to $g_{t\nu} = -0.8045$ and $g_{t\pi} = 2.3428$. The values of the occupation probabilities are taken from [20] as $u^2_{\frac{1}{2}\nu} = 0.63$, $u^2_{\frac{3}{2}\nu} = 0.86$, $u^2_{\frac{5}{2}\nu} = 0.81$ and $u^2_{\frac{3}{2}\pi} = 0.87$. Using these values the magnetic moment of the ground state of ^{196}Au becomes $\mu(2^-) = +0.5948\mu_N$ which is in almost perfect agreement with the experimental value of $+0.5906(5)\mu_N$.

Table 1 compares the experimental data with the theoretical predictions for the negative parity states. For the assignment to the experimental levels we follow Ref. [8]. To make conclusions from the comparison is very difficult due to the lack of knowledge on the multipolarities for most transitions which turn out to have a possible E2/M1 character. Only for the 212.8 keV transition from the first excited 4^- towards the 2^- groundstate a definite B(E2) value of 9.7(24) W.u. can be obtained. This ground-state transition is rather well reproduced by the theory with a value of 4.7 W.u. The same state shows also a more problematic decay to the $2^-, 3^-$ state at 162.6 keV. Theoretically, this state is assigned to be the second 2^- state. In this case an almost vanishing B(E2) value results to be compared to the observed B(E2) value of 13.2(13.2) W.u. However, it should be noted that the 50.2 keV transition has never been observed. This branch was deduced in Ref. [7] from missing intensities and under assumption of E2 multipolarity to be one thousand times smaller as the groundstate branch, which explains its 100% error bar. If the state instead would be the first 3^- state, theory gives $B(\mathrm{E2}; 4_1^- \to 3_1^-) = 16.0$ W.u. and $B(\mathrm{M1}; 4_1^- \to 3_1^-) = 0.0013\mu_N^2$. It would of great interest to confirm the existence of the 50.2 keV transition and to measure its multipolarity. For the decay of the 298.5 keV 1^- state we note that all M1 values are in the milli-Weisskopf unit (W.u.) domain, both in theory and experiment (assuming pure M1). In the unlikely case that they are all pure E2 the theory strongly under-

predicts the B(E2) values. For the positive parity states we observe experimentally very collective stretched E2 transitions between the yrast states.

5. Summary and conclusions

Using the ^{196}Pt(d, 2n)^{196}Au reaction, nanosecond lifetime measurements were performed by means of the pulsed-beam technique. The data were analyzed according to the centroid-shift method. As a result, one new lifetime has been determined and three known were re-measured. An upper limit of 0.4 ns can be set for the lifetimes of the other levels observed in the experiment. The data for the absolute transition probabilities are compared to the predictions of the extended supersymmetry for ^{196}Au. The comparison reveals a partial agreement, which can be considered as a moderate success for the theory describing the complicated structure of the odd–odd nucleus. Further work for a better experimental determination of the properties of the levels and γ-ray transitions in ^{196}Au is needed.

Acknowledgements

Support by the Deutsche Forschungsgemeinschaft unter grant JOL391/2-3 is acknowledged. P.P. is indebted to the National Science Fund at the Bulgarian Ministry of Education and Science for a financial support.

References

[1] P. Van Isacker, J. Jolie, K.L.G. Heyde, A. Frank, Phys. Rev. Lett. 54 (1985) 653.
[2] A. Metz, J. Jolie, G. Graw, R. Hertenberger, J. Gröger, C. Günther, N. Warr, Y. Eisermann, Phys. Rev. Lett. 83 (1999) 1542.
[3] F. Iachello, Phys. Rev. Lett. 44 (1980) 772.
[4] J. Jolie, U. Mayerhofer, T. von Egidy, H. Hiller, J. Klora, H. Lindner, H. Trieb, Phys. Rev. C 43 (1991) R16.
[5] J. Jolie, P.E. Garrett, Nucl. Phys. A 596 (1996) 234.
[6] D.D. Warner, R.F. Casten, A. Frank, Phys. Lett. B 180 (1986) 207.
[7] J. Gröger, J. Jolie, R. Krücken, C.W. Beausang, M. Caprio, R.F. Casten, J. Cederkall, J.R. Cooper, F. Corminboeuf, L. Genilloud, G. Graw, C. Günther, M. de Huu, A.I. Levon, A. Metz, J.R. Novak, N. Warr, T. Wendel, Phys. Rev. C 62 (2000) 064304.
[8] H.F. Wirth, G. Graw, S. Christen, Y. Eisermann, A. Gollwitzer, R. Hertenberger, J. Jolie, A. Metz, O. Möller, D. Tonev, B.D. Valnion, Phys. Rev. C 70 (2004) 014610.
[9] J. Barea, R. Bijker, A. Frank, Phys. Rev. Lett. 94 (2005) 152501.
[10] V.A. Ionescu, J. Kern, C. Nordmann, S. Olbrich, Ch. Rhême, Nucl. Instrum. Methods 163 (1979) 395.
[11] W. Andrejtscheff, M. Senba, N. Tsoupas, Z.Z. Ding, Nucl. Instrum. Methods 204 (1982) 123.
[12] P. Petkov, W. Andrejtscheff, L.K. Kostov, L.G. Kostova, Nucl. Instrum. Methods A 271 (1988) 617.
[13] P. Petkov, W. Andrejtscheff, S. Avramov, Nucl. Instrum. Methods Phys. Res. A 321 (1992) 259.
[14] Zh. Chunmei, W. Gongqing, T. Zhenlan, Nucl. Data Sheets 83 (1998) 145.
[15] A.M. Bruce, W. Gelletly, J. Lukasiak, W.R. Phillips, D.D. Warner, Phys. Lett. B 165 (1985) 43.
[16] F. Iachello, P. Van Isacker, The Interacting Boson–Fermion Model, Cambridge Univ. Press, 1991.
[17] J. Vervier, Riv. Nuovo Cimento 10 (9) (1987) 1.
[18] V. Paar, Nucl. Phys. A 331 (1979) 16.
[19] I. Hamamoto, Phys. Lett. B 61 (1976) 343.
[20] U. Mayerhofer, T. von Egidy, P. Durner, G. Hlawatsch, J. Klora, H. Lindner, S. Brant, H. Seyfarth, V. Paar, V. Lopac, J. Kopecky, D.D. Warner, R.E. Chrien, S. Pospisil, Nucl. Phys. A 492 (1989) 1.
[21] J. Jolie, Habilitation, Rijksuniversiteit Gent, 1992.